Journal of ASTM International, Vol. 6, No. 7
Paper ID JAI102406
Available online at www.astm.org

Mustafa Şahmaran,[1] *Mohamed Lachemi,*[2] *and Victor C. Li*[3]

Assessing the Durability of Engineered Cementitious Composites Under Freezing and Thawing Cycles

ABSTRACT: This paper reports the durability performance of non-air-entrained engineered cementitious composites (ECC) when subjected to freezing and thawing cycles. ECC is a newly developed, high-performance, fiber-reinforced, cementitious composite with substantial benefits both in terms of high ductility under uniaxial tensile loading and improved durability due to intrinsically tight crack width of less than 100 μm. To evaluate the frost durability of ECC, freezing and thawing testing in accordance with ASTM C666 Procedure A was conducted. The mass loss, pulse velocity change, and flexural parameters (ultimate deflection and flexural strength) of specimens subjected to freezing and thawing cycles were determined in the test. In addition, air-void parameters, in accordance with ASTM C457, modified point count method, and pore size distribution obtained by mercury intrusion porosimetry technique were studied. To analyze the influence of micro-fibers and high tensile strain capacity on the freezing and thawing durability of ECC, all of the above-mentioned properties were also investigated for a control ECC matrix (ECC without fibers). After 210 cycles of freezing and thawing, the control ECC matrix specimens were severely deteriorated, requiring removal from the test, but still exhibited better performance than the conventional non-air-entrained concrete, which would fail at much earlier cycles. On the other hand, ECC with fibers without air-entrainment had excellent resistance to cycles of freezing and thawing with minimal reduction in ultimate tensile strength and ductility. The observed superior frost durability of ECC over control ECC matrix in terms of lower weight loss, pulse velocity change, and higher flexural load and ductility can be attributed to the following reasons: Increase of pore volume larger than approximately 0.30 μm in diameter, intrinsically high tensile ductility and strength due to the presence of micro-poly-vinyl-alcohol fibers.

KEYWORDS: engineered cementitious composites (ECC), ductility, flexural strength, ECC under freezing and thawing cycles

Introduction

Concrete is the world's most widely used construction material. Historically, structural designers have primarily relied on concrete to carry compressive loads. However, in real field conditions, concrete is also subjected to tensile stresses due to loading and environmental effects including shrinkage (if the shrinkage is restrained), chemical attacks, and thermal effects. The tensile strength of concrete is only about 10 % of its compressive strength, and its brittle failure is of particular concern in structures. Durability is vitally important for all concrete structures, and it can be associated with the appearance of cracks when concrete is subjected to tensile stresses.

In recent years, efforts to modify the brittle nature of ordinary concrete have resulted in ultra-high-performance fiber-reinforced cementitious composites, which are characterized by tensile strain-hardening after first cracking. Depending on their composition, their tensile strain capacity can be up to several hundred times that of normal and fiber-reinforced concrete. Engineered cementitious composite (ECC) is a fiber-reinforced cement-based composite material that is micro-mechanically tailored by the addition of short fibers to achieve high ductility and multiple cracking under tensile and shear loading [1–6]. Unlike ordinary concrete materials, ECC strain-hardens after first cracking, similar to a ductile metal, and demonstrates a strain capacity 300–500 times greater than normal concrete. Figure 1 shows a typical uniaxial tensile stress-strain curve of an ECC containing 2 % by volume of poly-vinyl-alcohol fiber (PVA fiber). The characteristic strain-hardening after first cracking is accompanied by sequential development of mul-

Manuscript received March 5, 2009; accepted for publication May 26, 2009; published online August 2009.
[1] Dept. of Civil Engineering, Gaziantep Univ., Gaziantep, 27310,Turkey, e-mail: sahmaran@gantep.edu.tr
[2] Dept. of Civil Engineering, Ryerson Univ., Toronto, M5B 2K3Canada, e-mail: mlachemi@ryerson.ca
[3] Dept. of Civil and Environmental Engineering, The Univ. of Michigan, MI 48109-2125 (Corresponding author), e-mail: vcli@umich.edu

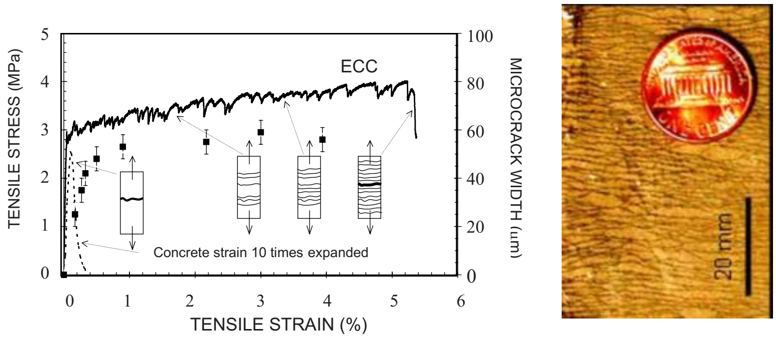

FIG. 1—*Typical uniaxial tensile stress-strain curve and crack width development of PVA-ECC.*

tiple micro-cracking and a tensile strain capacity 300–500 times that of normal concrete. Crack width development during inelastic straining is also shown in Fig. 1. Even at large imposed deformations, crack widths of ECC remain small; less than 80 µm. This tight crack width is self-controlled and, whether the composite is used in combination with conventional reinforcement or not, it is a material characteristic independent of the amount of reinforcing bars. The tight crack width of ECC is important to the durability of ECC structures as the tensile ductility is to the structural safety at ultimate limit state. Under severe bending load, an ECC beam deforms similar to a ductile metal plate through plastic deformation (Fig. 2). In compression, ECC materials exhibit compressive strengths similar to high strength concrete (e.g., greater than 60 MPa) [7]. These properties, along with the relative ease of production including self-consolidation casting [8,9] and shotcreting [10], make ECC materials suitable for various civil engineering applications. ECC is currently emerging in full-scale structural applications [11,12].

Much infrastructures in North America and Turkey are located in regions with severe environmental conditions, where alternate freezing and thawing can seriously affect material/structure integrity. The limited field performance and preliminary freeze-thaw durability study of non-air-entrained ECC indicates that it has a superior freezing and thawing resistance [13–15]. As one of the first field applications of ECC in United States, a concrete bridge deck patch was completed in cooperation with the Michigan Department of Transportation (MDOT) in 2002. A complete summary of this work has been outlined by Li and Lepech [15]. During this work, one section of a deteriorated bridge deck was repaired with ECC while the remaining portion was repaired with a commercial concrete patching material commonly used by the MDOT. This repair scenario allowed for a unique ECC/concrete comparison subjected to identical environmental and traffic loads. The concrete repair material used was a pre-packaged, commercially available repair mortar. At this writing, the repaired bridge deck has experienced more than eight complete Michigan winter cycles of freezing and thawing, in addition to live loads. While the ECC patch repair has survived

FIG. 2—*Response of ECC beam after 300 freezing and thawing cycles under flexural loading.*

TABLE 1—*Chemical composition and physical properties of cement and fly ash.*

Chemical Composition, %	Cement	Fly Ash
CaO	61.80	5.57
SiO_2	19.40	59.50
Al_2O_3	5.30	22.20
Fe_2O_3	2.30	3.90
MgO	0.95	···
SO_3	3.80	0.19
K_2O	1.10	1.11
Na_2O	0.20	2.75
Loss on ignition	2.10	0.21
Physical properties		
Specific gravity	3.15	2.18
Retained on 45 μm (0.002 in.), %	12.9	9.6
Water requirement, %	···	93.4

in this combined loading environment with minor micro-cracking limited to less than 50 μm, the concrete repair portion has developed localized cracks in excess of 3.5 mm wide and required re-repair in 2005.

A proper air-void system must be maintained in normal concrete to achieve superior freezing and thawing resistance [16]. In the case of ECC, the available information is very limited, but it seems to indicate that in addition to the air-void system, other parameters such as high tensile strain capacity and strain-hardening behavior are important for resisting cycles of freezing and thawing and are affected by the presence of micro-fibers. It is therefore essential to further investigate the reasons behind the excellent frost resistance of ECC. This study was undertaken to comprehensively investigate the freezing and thawing durability of non-air-entrained standard ECC mixture (M45). The resulting data is important in view of the growing use of ECC, especially for highway pavements, airport pavements, and bridge decks in cold climate regions.

To evaluate the freeze-thaw durability of ECC, freezing and thawing testing in accordance with ASTM C666 Procedure A was conducted. The mass loss, pulse velocity change, and flexural parameters (ultimate deflection and flexural strength) of specimens subjected to freezing and thawing cycles were determined. In addition, air-void parameters, in accordance with ASTM C457, modified point count method, and pore size distribution obtained by mercury intrusion porosimetry method were studied. To analyze the influence of micro-fibers and excellent tensile performance (high tensile strain capacity, strain-hardening, and multiple-cracking behaviors) on the freezing and thawing durability of ECC, all of the above-mentioned properties were also investigated for an ECC matrix (ECC without fibers).

Experimental Studies

Materials, Mixture Proportions, and Basic Mechanical Properties

The materials used in the production of standard ECC mixtures were Type-I Portland cement (C), Class-F fly ash (FA) with a lime content of 5.6 %, micro-silica sand with an average and maximum grain size of 110 and 250 μm, respectively, water, PVA fibers, and a polycarboxylic-ether type high-range water reducing (HRWR) admixture. Chemical composition and physical properties of Portland cement and FA are presented in Table 1. The PVA fibers with a diameter of 39 μm and a length of 8 mm are purposely manufactured with a tensile strength of 1620 MPa, elastic modulus of 42.8 GPa, maximum elongation of 6.0 %, and the ability to strain-harden [3]. The PVA fiber tends to rupture instead of pull out in a cementitious matrix, as a result of the strong chemical bonding with cement due to the presence of the hydroxyl group in its molecular chains [3]. This high chemical bonding has a tendency to lead to fiber rupture and limits the tensile strain capacity of the resulting composite. For this reason, the surface of the PVA fibers is coated with a proprietary hydrophobic oiling agent of 1.2 % by mass to tailor the interfacial properties between fiber and matrix for strain-hardening performance.

TABLE 2—*Mixture properties of ECC.*

	ECC (M45) with PVA	ECC Matrix Without PVA
FA/C	1.2	1.2
W/CM[a]	0.27	0.27
Water (W), kg/m^3	326	326
Cement (C), kg/m^3	558	558
Fly ash (FA), kg/m^3	669	669
Sand (S), kg/m^3	446	446
Fiber (PVA), kg/m^3	26	⋯
HRWR, kg/m^3	2.30	2.30
14 day compressive strength, MPa	39.2	36.1
28 day compressive strength, MPa	62.5	60.3

[a]CM denotes cementitious materials (cement+fly ash).

Standard ECC mixture (M45) with a fly ash-cement ratio (FA/C) of 1.2 by mass was used in this investigation, details of which are given in Table 2. To analyze the influence of micro-fibers and high tensile strain capacity on the freezing and thawing durability of ECC, ECC matrix (ECC without PVA fibers) was also studied. ECC and ECC matrix were prepared in a standard paddle mixer at a constant amount of cementitious material and constant water to cementitious material ratio (W/CM) of 0.27. All ECC and ECC matrix materials used in this study contain no air-entraining admixture (AEA) and show self-consolidating flow behavior in the fresh state. Previous studies demonstrated that concretes containing HRWR often tend to have air-voids that are larger than those in conventional concrete [17–20]. Such air-void systems tend to be less stable and have larger spacing factors. Since the same dosage of HRWR is used in the production of ECC matrix and ECC, HRWR admixture cannot be a factor responsible for the great differences in the frost durability of ECC and ECC matrix, which will be discussed in the next section.

The compressive strength test results of the ECC and ECC matrix without fibers and the ultimate tensile strain capacity of ECC are listed in Tables 2 and 3, respectively. The compressive strength was computed as an average of three 50 mm cubic specimens. To characterize the direct tensile behavior of the ECC mixtures, $200 \times 75 \times 13\ mm^3$ coupon specimens were used. Direct tensile tests were conducted under displacement control at a loading rate of 0.005 mm/s. The typical tensile stress-strain curves of the ECC mixtures at 14 and 28 days are shown in Fig. 3. As seen from Table 3, the ECC composite exhibited a strain capacity of 2.7 % at 28 days. The strain capacity measured at 28 days of age is slightly lower than the 14 day strain capacity (Fig. 3 and Table 3) but within the acceptable variability; and the strain capacity exceeding 2.5 % is acceptable. Previous studies demonstrated that the tensile strain capacity seems to stabilize after 28 days. This time dependent stabilization can be ascribed to the increase in fiber/matrix interface properties and matrix toughness associated with the continued cement hydration process [14].

Specimen preparation and testing

From each mixture, eight $400 \times 100 \times 75\ mm^3$ prisms were prepared for the freezing and thawing test and determination of air-void characteristics. All specimens were cast in one layer without any compaction, demolded at the age of 24 h, and moist cured in lime-saturated water at $23 \pm 2°C$ for 13 days. Fourteen days after casting, the beam specimens were moved into the freeze-thaw chamber in accordance with ASTM C666 Procedure A and subjected to between five and six freezing and thawing cycles in a 24 h period. The average flexural parameters (ultimate deflection and flexural strength) of the specimens were obtained by testing four companion samples prior to the freezing and thawing cycles. Changes in pulse velocity and mass loss were measured at each interval of nominally 30 cycles of freezing and thawing. The

TABLE 3—*Uniaxial tensile properties of ECC specimens at 28 days.*

Age	Tensile Strain, %	Tensile Strength, MPa	Residual Crack Width, μm
14 days	2.9 ± 0.2	4.6 ± 0.5	~60
28 days	2.7 ± 0.2	5.1 ± 0.3	~48

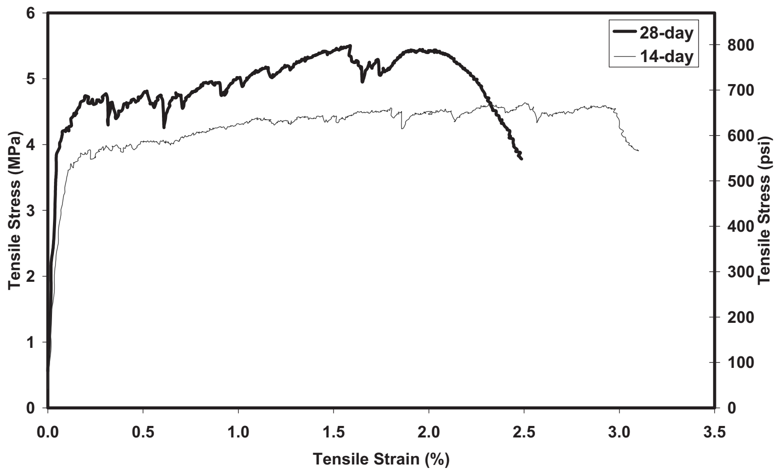

FIG. 3—*Typical tensile stress-strain response of standard ECC mixture (M45).*

number of cycles to failure for the specimens was also recorded at the time the sample fractured or split into two parts. At the end of 300 freeze-thaw cycles, surviving specimens were tested under four-point bending load with a span length of 355 mm and a height of 75 mm to determine their residual flexural performances, and their load-deflection curves were recorded. Three freeze-thaw specimens were tested for each mixture.

The air-void parameters of hardened ECC and ECC matrix (without fiber) were determined by modified point count method according to ASTM C457. Mercury intrusion porosimetry was also used to characterize the pore size distribution of the ECC and ECC matrix. An instrument capable of producing pressures up to 414 MPa and assuming a contact angle of 130° was used for pore size distribution analysis by the mercury intrusion method. Specimens were dried to constant weight at 50°C prior to testing. All tests included at least two identical specimens tested at the same time.

Results and Discussions

Air-void parameters

The results of the determination of air-void characteristics of the hardened concrete (air content, specific surface and spacing factor), according to ASTM C457, are shown in Table 4, along with the air content measured on the fresh state (as measured by ASTM C231), and total intruded porosity values obtained with the mercury intrusion porosimetry technique. The freeze-thaw durability of concrete has a close relationship with its air-void parameters. The American Concrete Institute (ACI) recommends that frost-resistant concrete should have a calculated spacing factor of less than 0.2 mm and a specific surface greater than 24 mm^{-1} [21].

As seen in Table 4, although no AEA was added to the ECC and ECC matrix mixtures, the air contents of these mixtures in the fresh state gave values of 7.3 % and 5.9 %, and in the hardened state, as measured by ASTM C457, gave values of 8.2 % and 7.3 %, respectively. These amounts seemed to be adequate for freeze-thaw durability [21]. The higher air content in these mortar mixtures may be due to the lack of coarse aggregate and the higher viscosity of the mortar matrix during the fresh state [22]; the fine particles

TABLE 4—*Air-void characteristics and porosity.*

	ECC (M45) with PVA	ECC matrix without PVA
Fresh air content (%)	7.3	5.9
Hardened air content (%)	8.2	7.3
Specific surface (mm^{-1})	25.6	53.0
Spacing factor (mm)	0.241	0.129
Total intruded porosity (%)	23.7	19.2
Volume of pores >0.30 μm diameter (%)	5.0	0.75

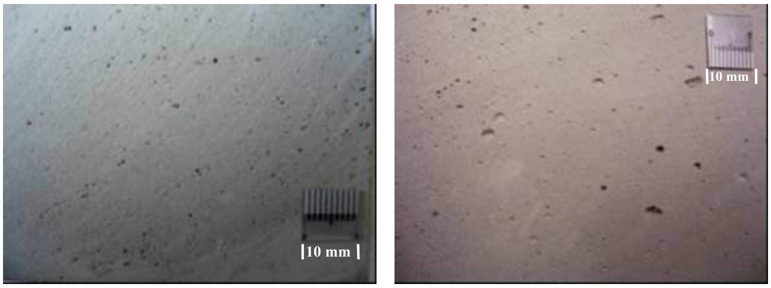

ECC matrix (without PVA fiber)

ECC (with PVA fiber)

FIG. 4—*Typical air-voids in a non-air-entrained ECC specimens (without and with fiber).*

and high viscosity tend to prevent some of the air bubbles from rising to the surface during placing operations. Moreover, the air contents measured during the fresh state of the ECC mixture show that this phenomenon is amplified after the addition of PVA fiber to the mixtures (Table 2). When PVA is added to the ECC matrix, it increases the viscosity of the fresh ECC mixture compared to the ECC matrix [23], which further increases the amount of entrapped air-voids inside the matrix.

In the case of hardened ECC, it is interesting to note that the addition of the PVA fiber can result in a significant increase in spacing factor (see Table 4). Moreover, specific surface is significantly higher for ECC matrix, which indirectly implies that the average bubble size is smaller in ECC matrix. This is likely due to the fact that the randomly distributed PVA fibers could possibly form a network that provides a path for the air bubbles to coalesce, thus creating large entrapped air-voids instead of finely distributed air-voids, which can be clearly seen in Fig. 4. It would be necessary to further investigate the reasons behind the increase in spacing factor and reduction in specific surface with the addition of PVA fiber.

Although the spacing factor value (0.241 mm) and specific surface value (25.6 mm^{-1}) of ECC slightly exceed the generally acceptable value of 0.200 mm and 25 mm^{-1} for good freeze-thaw durability, the apparent lack of an ideal air-void characteristic has not adversely affected resistance when ECC is subjected to freezing and thawing cycles, as discussed in the following section.

The total mercury intruded porosities for the various pastes are shown in Table 4. Typical pore size distribution curves are shown in Fig. 5 for the ECC and ECC matrix (without fiber) samples. The ECC exhibited a higher total porosity when compared with the ECC matrix. However, total porosity is not a good indicator of quality (i.e., freeze-thaw durability) since very small gel pores would not negatively influence concrete durability [24]. The radius and size distribution of pores determine the freezing point of pore solution and the amount of ice formed in pores [25]. According to current literature, while a uniform relationship between freeze-thaw resistance and pore size distribution obtained by mercury intrusion technique has not been found, in general, a larger volume of coarse pores (greater than approximately 0.30 μm diameter [26–31]) results in higher freeze-thaw resistance. The volumes of pores larger than 0.30 μm diameter are also given in Table 4, which shows that due to PVA fiber incorporation, there is a

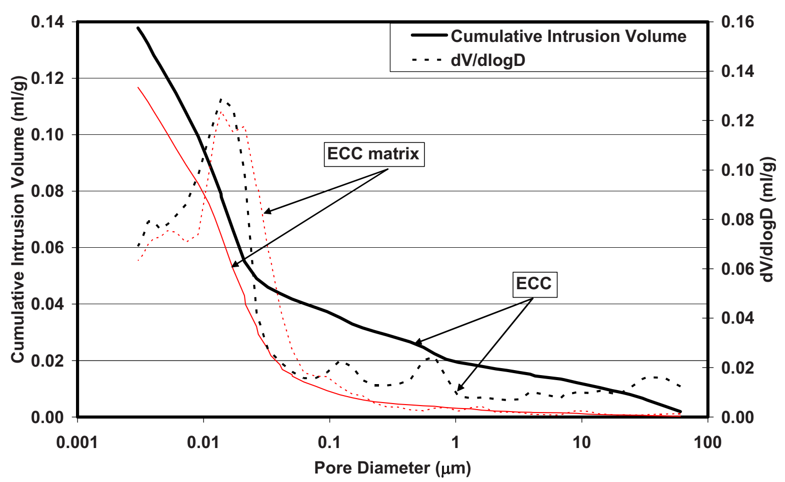

FIG. 5—*Cumulative pore size distributions of non-air-entrained ECC specimens (without and with fiber).*

TABLE 5—*Freezing and thawing resistance of ECC and ECC matrix.*

	ECC matrix without PVA	ECC (M45) with PVA
Number of cycles completed	210	300
Change in mass (%)	−7.3	−1.3
Pulse velocity change (%)	−30.9	−2.2

significant difference in pore size distribution, mainly in sizes larger than 0.30 μm diameter. The addition of PVA fiber to the matrix significantly increased the volume of these large-size pores and the total porosity, which is favorable to improved frost resistance.

Freezing and Thawing Resistance

The deterioration of specimens during the freezing and thawing cycles was assessed by the computation of mass loss. To measure the internal damage caused by freezing and thawing cycles, the changes in pulse velocity through a prism were also measured. Normally, ASTM C666 specifies the use of the resonant frequency method, not the pulse velocity method. However, previous studies have shown that pulse velocity test method can also be used to measure the deterioration of specimens during freezing and thawing cycles [32].

The freeze-thaw durability test results are summarized in Table 5. Figure 6 shows the data for the relative pulse velocity change (V_i/V_0) and relative mass change (M_i/M_0) with the number of freezing and thawing cycles. V_i and M_i are the pulse velocity and mass, respectively, after a specific number of freezing and thawing cycles, and V_0 and M_0 are initial pulse velocity and mass, respectively, prior to any freezing and thawing cycles. As seen in Fig. 6, the mass and pulse velocity losses of ECC matrix increase with the number of freeze-thaw cycles. After 210 cycles, the ECC matrix specimens had severely deteriorated [Fig. 7(*a*)], requiring removal from the freeze-thaw machine, as mandated by the testing standard. However, as seen in Table 5, the ECC prisms showed excellent performance when exposed to freezing and thawing cycles, even after 300 cycles. A maximum of only 1.3 % and 2.2 % mass and pulse velocity losses, respectively, were measured for the ECC specimens. This can also be observed in Fig. 6, where the relationship between relative pulse velocity/relative mass loss and number of freezing and thawing cycles is shown for ECC specimens that were subjected to 300 cycles. At the end of 300 cycles, very little scaling was observed on the ECC prism surface [Fig. 7(*b*)].

There are a number of possible explanations for the excellent performance of these non-air-entrained ECC samples. A proper air-void system is needed in normal concrete to avoid internal cracking due to freezing and thawing cycles. As discussed in the preceding section, the pore size distributions of ECC matrix are much finer (i.e., fewer coarse pores) than ECC. To make a general conclusion regarding the influence of pore size distribution on frost resistance, large pores (generally larger than 0.3 μm in diameter) are beneficial to frost resistance of concrete, whereas small and intermediate pores are detrimental (see "Air-Void Parameters" section).

Another possible reason for the ECC's excellent frost resistance, which is favored by the authors, can be attributed to its superior tensile properties (see "Flexural Performance" section). It is well known that upon freezing, water in capillary pores expands. If the required volume is greater than the space available, the pressure build-up could reach the tensile strength of the material, resulting in local micro-crack formation, brittle rupture and scaling. Therefore, the high tensile strength—and particularly fracture resistance in ECC—could lead to its higher frost resistant characteristic. The influence of micro-fiber addition

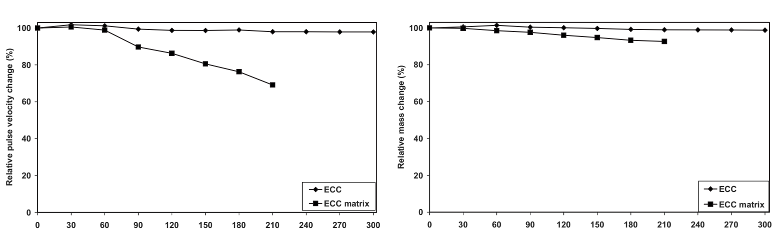

FIG. 6—*Relative pulse velocity and mass loss changes as a function of number of freezing and thawing cycles.*

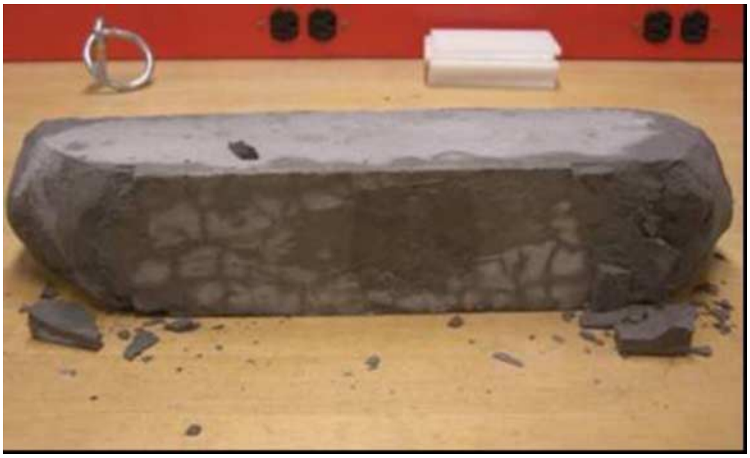

(a) ECC matrix (ECC without fiber) after 210 freezing and thawing cycles

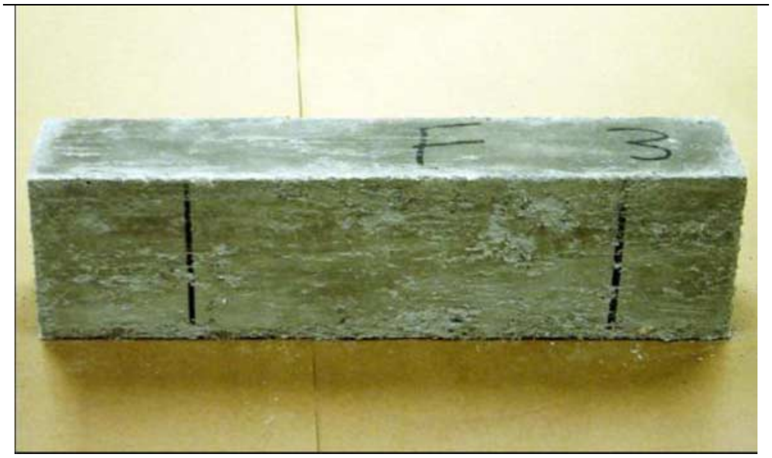

(b) ECC (with fiber) after 300 freezing and thawing cycles

FIG. 7—*ECC specimen surface appearance after freeze-thaw cycles.*

on frost resistance of conventional concrete has also been examined by other researchers [33,34] and is in agreement with what is found in this study. When PVA fiber is incorporated into ECC matrix, both the pressure-releasing effect [due to larger pore size (see "Air-Void Parameters" above)] and the crack-resisting effect contribute to the ability to resist deterioration during freezing and thawing cycles. Further experimental studies are needed to clearly understand the relative contributions of each factor discussed above on the frost resistance of ECC.

Flexural Performance

Table 6 provides the test results in terms of flexural strength (modulus of rupture) and ultimate mid-span beam deflection at peak stress before and after freezing and thawing deterioration. Typical flexural stress-mid-span deflection curves of ECC and ECC matrix (without fiber) specimens before and after freezing and thawing deterioration are shown in Fig. 8. Each result in Table 6 is an average of three to four specimens.

As seen in Table 6, the average flexural strengths were 4.42 and 11.44 MPa for ECC and ECC matrix, respectively, prior to freezing and thawing cycles. The ECC shows a substantially higher ultimate flexural strength than the ECC matrix. This may be attributed to the fact that micro-fibers inhibit the localization of micro-cracks into macro-cracks and consequently, the tensile strength of the ECC matrix increases with the formation of multiple micro-cracks during inelastic deformation. In all of the ECC specimens with/without freezing and thawing deterioration, prismatic specimens showed multiple cracking behaviors with

TABLE 6—*Flexural properties of ECC (M45) prisms before and after 300 freeze-thaw cycles.*

Specimen type		Ultimate Deflection, mm	Flexural Strength, MPa	Residual Crack Width, μm
Cured 21 days moist curing	ECC matrix (without fiber)	0.68 [0.24]	4.42 [0.79]	···
	ECC (with fiber)	5.23 [0.16]	11.44 [0.54]	~61 [~13]
Subjected to 300 freezing and thawing cycles	ECC (with fiber)	4.91 [0.40]	9.70 [0.19]	~70 [~28]

Note: Numbers in brackets are standard deviations.

small crack spacing and tight crack widths (<0.1 mm). The first crack started inside the mid-span at the tensile face. The flexural stress increased at a slower rate, along with the development of multiple cracks with small crack spacing and tight crack widths. Micro-cracks developed from the first cracking point and spread out in the mid-span of the flexural beam, as shown in Fig. 9. Bending failure in the ECC occurred when the fiber-bridging strength at one of the micro-cracks was reached, resulting in localized deformation

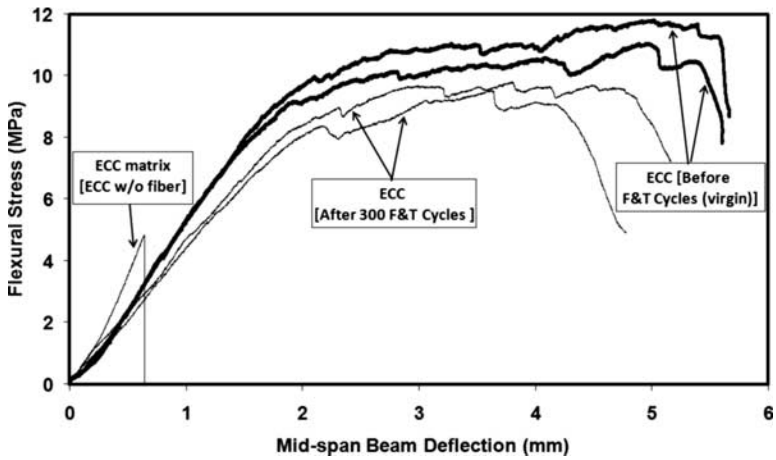

FIG. 8—*Effect of freezing and thawing cycles on flexural behavior of ECC.*

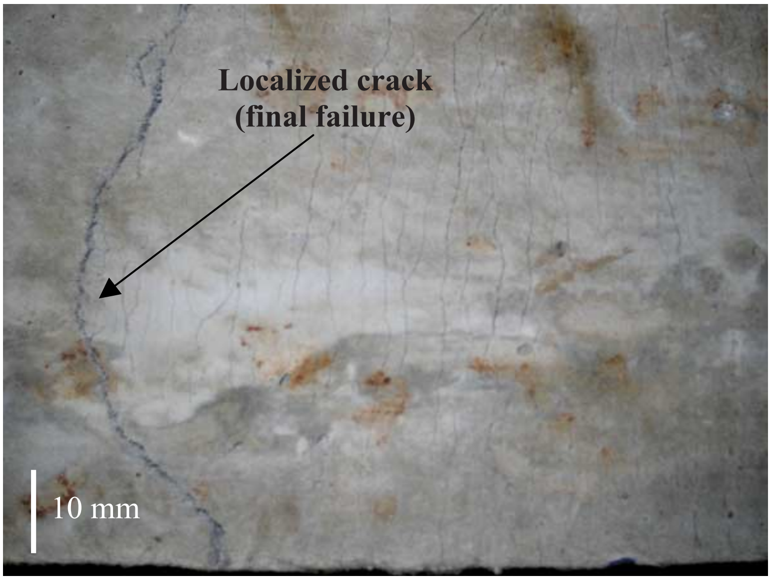

FIG. 9—*Typical multiple crack pattern on the bottom tensile surface of ECC beam specimen after flexure load applications.*

(Fig. 9) once the modulus of rupture was approached. On the other hand, because of their low tensile properties and brittle nature, the ECC matrix beams failed catastrophically with a single crack under the four-point bending test.

Flexural stress-mid-span deflection curves obtained for the ECC prism specimens exposed to 300 freezing and thawing cycles are shown in Fig. 8. The typical flexural stress-deflection curves of ECC specimens after frost deterioration show that the influence of 300 freezing and thawing cycles on the flexural stress-mid-span deflection curves is fairly minor. This result is consistent with the earlier results of mass and pulse velocity losses of ECC specimens after 300 freezing and thawing cycles (Fig. 6). As seen in Fig. 8, the first-cracking strength of the ECC specimens after cyclic exposure falls below the first-cracking strength of the virgin ECC specimens (control specimens prior to freezing and thawing cycles). The slope of the load-deflection curve represents the stiffness of the beams; Fig. 8 shows that the slope decreases with frost deterioration, thereby indicating a slight reduction in the stiffness of the ECC beams. Nevertheless, no significant reduction in the flexural strength and deflection capacities of the ECC specimens exposed to 300 freezing and thawing cycles was detected.

It should be noted that the residual ultimate flexural load-deflection curves of frost deteriorated ECC beams (Fig. 8) obtained following induced accelerated freeze-thaw cycling (up to six freezing and thawing cycles were achieved in a 24 h period) provide a conservative estimate of their residual flexural properties in actual structures. These accelerated deterioration periods are equivalent to a time span of many years in real structures, even those located in regions with harsh winters. This difference in accelerated and normal frost deterioration periods should have a significant influence on the residual flexural properties of ECC because in the long term, deterioration in ECC as a result of freezing and thawing cycles can easily be closed due to a self-healing process [31]. Thus the flexural performances of ECC summarized in Table 6 are underestimated.

Table 6 summarizes the flexural strength (modulus of rupture) and total mid-span deflection at the peak stress of ECC specimens exposed to 300 freezing and thawing cycles. The total deflection of the ECC beam, which reflects material ductility, exposed to 300 freezing and thawing cycles is 4.91 mm, which is slightly lower than that of ECC mixture prior to undergoing freezing and thawing cycles. Compared to control ECC specimens cured in laboratory air, the test results (Table 6) indicate that the ECC specimens exposed to freezing and thawing cycles showed reductions of nearly 15 % in flexural strength at the end of 300 cycles; this may be attributed to the effects of damage on the fiber/matrix interface and matrix micro-cracking.

Table 6 also shows the residual crack width of ECC mixtures at different ages. The term "residual crack width" indicates that crack width was measured from the unloaded specimen after the four-point flexural test by using a portable microscope with an accuracy of 5 μm. Both frost-deteriorated and virgin ECC specimens reveal saturated multiple cracking (Fig. 9) with crack width at ultimate flexural load limited to below 100 μm. Crack width control is of primary importance for many reinforced concrete applications since it is believed that there is a close relationship between mean or maximum crack widths and the durability of the structure. Moreover, the lower magnitude of the crack width is expected to promote self-healing behavior, and thus the transport properties in cracked composites [35–38]. In terms of permeability and diffusion, crack width less than 100 μm generally behaves like sound concrete [35,39]. Based on experimental results, Şahmaran et al. [35], Evardsen [40], and Reinhardt and Jooss [41] proposed that cracks with a width below 100 μm can be easily closed by a self-healing process. Consequently, in the serviceability limit state, a mean or maximum crack width less than about 0.1 mm is usually prescribed [39,40].

Conclusion

In this study, the frost resistance of ECC assessed by alternate freezing and thawing cycles in accordance with ASTM C666 Procedure A, air-void parameters determined by the modified point count method (ASTM C457), and the pore size distribution obtained by mercury intrusion porosimetry technique were compared with ECC matrix (ECC without PVA fiber). While the control ECC matrix specimens rapidly failed in freezing and thawing (ASTM C666 Procedure A), ECC easily survived 300 cycles. Apart from the slight reduction in ultimate flexural strength and ductility, the test results presented in this study confirm that ECC provides excellent frost protection compared to ECC matrix. Despite a slight reduction in ductility and flexural strength, after 300 freezing and thawing cycles, ECC samples are found to retain tensile ductility more than a few hundred times, with residual crack width less than 100 μm on reloading, which is that of normal concrete and fiber-reinforced concrete with no environmental exposure. Further, it is important to note that this superior durability performance of ECC under freezing and thawing cycles was achieved without deliberate air-entrainment. For this reason, it is expected that the ECC investigated is suitable for long-term application under severe environmental conditions of alternate freezing and thawing cycles, if the structure is designed based on long-term mechanical properties.

Experimental evidence indicates that the excellent frost durability of ECC was due to the increase of pore volume larger than approximately 0.30 μm diameter, and intrinsically high tensile ductility and strength attained as a result of micro-mechanically based design principles. The presence of micro-PVA fibers critically contributes to the higher crack resistance and larger pore volume, and resulting pressure-releasing effects under freeze-thaw conditions.

Acknowledgments

The authors gratefully acknowledge the Scientific and Technical Research Council (TUBITAK) of Turkey provided under Project No. MAG-108M495 and the financial assistance of the Natural Sciences and Engineering Research Council (NSERC) of Canada, the Canada Research Chair Program. This international research collaboration was enhanced by a CI-Team grant (Grant No. OCI 0636300) from the United States National Science Foundation (NSF).

References

[1] Li, V. C., "Engineered Cementitious Composites—Tailored Composites Through Micromechanical Modeling," *Fiber Reinforced Concrete: Present and the Future*, N. Banthia, A. Bentur, and A. Mufti, Eds., Canadian Society for Civil Engineering, Montreal, 1997, pp. 64–97.

[2] Li, V. C., "On Engineered Cementitious Composites (ECC) – A Review of the Material and Its Applications," *J. Adv. Concr. Technol.*, Vol. 1, 2003, pp. 215–230.

[3] Li, V. C., Wang, S., and Wu, C., "Tensile Strain-Hardening Behavior of PVA-ECC," *ACI Mater. J.*, Vol. 98, 2001, pp. 483–492.

[4] Li, V. C., Mishra, D. K., and Wu, H. C., "Matrix Design for Pseudo Strain-Hardening Fiber Reinforced Cementitious Composites," *RILEM J. Mater. Struct.*, Vol. 28, 1995, pp. 586–595.

[5] Maalej, M., Li, V. C., and Hashida, T., "Effect of Fiber Rupture on Tensile Properties of Short Fiber Composites," *J. Eng. Mech.*, Vol. 121, 1995, pp. 903–913.

[6] Li, V. C., Wu, C., Wang, S., Ogawa, A., and Saito, T., "Interface Tailoring for Strain-Hardening PVA-ECC," *ACI Mater. J.*, Vol. 99, 2002, pp. 463–472.

[7] Lepech, M. and Li, V. C., "Large Scale Processing of Engineered Cementitious Composites," *ACI Mater. J.*, Vol. 105, 2008, pp. 358–366.

[8] Kong, H. J., Bike, S., and Li, V. C., "Development of a Self-Consolidating Engineered Cementitious Composite Employing Electrosteric Dispersion/Stabilization," *Cem. Concr. Compos.*, Vol. 25, 2003, pp. 301–309.

[9] Kong, H. J., Bike, S., and Li, V. C., "Constitutive Rheological Control to Develop A Self-Consolidating Engineered Cementitious Composite Reinforced with Hydrophilic Poly(Vinyl Alcohol) Fibers," *Cem. Concr. Compos.*, Vol. 25, 2003, pp. 333–341.

[10] Kim, Y. Y., Kong, H. J., and Li, V. C., "Design of Engineered Cementitious Composite (ECC) suitable for wet-mix shotcreting," *ACI Mater. J.*, Vol. 100, 2003, pp. 511–518.

[11] Kunieda, M. and Rokugo, K., "Recent Progress on HPFRCC in Japan," *J. Adv. Concr. Technol.*, Vol. 4, 2006, pp. 19–33.

[12] Li, V. C., Lepech, M., and Li, M., "Field Demonstration of Durable Link Slabs for Jointless Bridge Decks Based on Strain-Hardening Cementitious Composites," *Report No.* RC-1438, Michigan Department of Transportation (DOT), 2005.

[13] Li, V. C., Fischer, G., Kim, Y. Y., Lepech, M., Qian, S., Weimann, M., and Wang, S., "Durable Link Slabs for Jointless Bridge Decks Based on Strain-Hardening Cementitious Composites," *Report No.* RC-1438, Michigan Department of Transportation (DOT), 2003.

[14] Lepech, M. D. and Li, V. C., "Long Term Durability Performance of Engineered Cementitious Composites," Int. J. Restor. Build. Monuments, Vol. 12, 2006, pp. 119–132.

[15] Li, V. C. and Lepech, M. "Crack Resistant Concrete Material for Transportation Construction," *TRB 83rd Annual Meeting, Washington, D.C., Compendium of Papers* (CD ROM), Transportation Research Board, Washington, D.C., <, 2004, Paper No. 04–4680.

[16] Pigeon, M. and Pleau, R., *Durability of Concrete in Cold Climates*, Chapman & Hall, London, 1995.

[17] Siebel, E., "Air-Void Characteristics and Freezing and Thawing Resistance of Superplasticized Air-Entrained Concrete with High Workability," *Superplasticizers and Other Chemical Admixtures in Concrete, SP-119*, American Concrete Institute, Farmington Hills, MI, 1989, pp. 297–319.

[18] Saucier, F., Pigeon, M., and Plante, P., "Air-Void Stability, Part III: Field Tests of Superplasticized Concretes," *ACI Mater. J.*, Vol. 87, 1990, pp. 3–11.

[19] Pigeon, M., Plante, P., and Plante, M., "Air-Void Stability, Part I: Influence of Silica Fume and Other Parameters," *ACI Mater. J.*, Vol. 86, 1989, pp. 482–490.

[20] Pigeon, M., Saucier, F., and Plante, P., "Air-Void Stability, Part IV: Retempering," *ACI Mater. J.*, Vol. 87, 1990, pp. 252–259.

[21] ACI Committee 345, "Proposed Revision of ACI 345–74: Standard Practice for Concrete Highway Bridge Deck Construction," *Concr. Int.*, Vol. 3, 1981, pp. 19–53.

[22] Powers, T. C., "Frost Resistant Concrete," *J. PCA Res. Dev. Lab*, Vol. 6, 1964, pp. 19.

[23] Yang, E., Şahmaran, M., Yang, Y., and Li, V. C., "Rheological Control in the Production of Engineered Cementitious Composites," *ACI Mater. J.* Vol. 106, 2009 (in press).

[24] Hooton, R. D., "Influence of Silica Fume Replacement of Cement on Physical Properties and Resistance to Sulfate Attack, Freezing, and Thawing, and Alkali–Silica Reactivity," *ACI Mater. J.*, Vol. 90, 1993, pp. 143–151.

[25] Cai, H. and Liu, X., "Freeze–Thaw Durability of concrete: Ice Formation Process in Pores," *Cem. Concr. Res.*, Vol. 28, 1998, pp. 1281–1287.

[26] Litvan, G. G., "Air Entrainment in the Presence of Superplasticizers," *ACI Mater. J.*, Vol. 80, 1983, pp. 326–331.

[27] Koh, Y. and Kamada, E., "The Influence of Pore Structure of Concrete Made with Absorptive Aggregates on the Frost Durability of Concrete," *Proceedings RILEM/IUPAC International Symposium on Pore Structure and Properties of Materials*, Vol. 11, Artia, Prague, 1973, pp. F45–F62.

[28] Cebeci, O. Z., "Pore Structure of Air-Entrained Hardened Cement Paste," *Cem. Concr. Res.*, Vol. 11, 1981, pp. 257–265.

[29] Litvan, G. G. and Sereda, P. J., "Particulate admixture for Enhanced Freeze–Thaw Resistance of Concrete," *Cem. Concr. Res.*, Vol. 8, 1978, pp. 53–60.

[30] Lange, H. and Modry, S., "Determination of the Frost Resistance of Limestone Aggregates in The Light of Porosity Investigation," *Proceedings of the RILEM Symposium on Durability of Concrete*, Building Research Institute, Prague, 1969, pp. B129–B168.

[31] Şahmaran, M. and Li, V. C., "De-Icing Salt Scaling Resistance of Mechanically Loaded Engineered Cementitious Composites," *Cem. Concr. Res.*, Vol. 37, 2007, pp. 1035–1046.

[32] Cohen, M. D., Zhou, Y., and Dolch, W. L., "Non-Air-Entrained High Strength Concrete—Is It Frost Resistant?," *ACI Mater. J.*, Vol. 89, 1992, pp. 406–415.

[33] Pigeon, M., Azzabi, M., and Pleau, R., "Can Microfibers Prevent Frost Damage?," *Cem. Concr. Res.*, Vol. 26, 1996, pp. 1163–1170.

[34] Deja, J., "Freezing and De-Icing Salt Resistance of Blast Furnace Slag Concretes," *Cem. Concr. Compos.*, Vol. 25, 2003, pp. 357–361.

[35] Şahmaran, M., Li, V. C., and Li, M., "Transport Properties of Engineered Cementitious Composites Under Chloride Exposure," *ACI Mater. J.*, Vol. 104, 2007, pp. 604–611.

[36] Şahmaran, M. and Li, V. C., "Influence of Microcracking on Water Absorption and Sorptivity of ECC," *Mater. Struct.* Vol. 42, 2009, pp. 593–603.

[37] Lepech, M. D. and Li, V. C., "Water Permeability of Cracked Cementitious Composites," *Paper 4539 of Compendium of Papers* (CD ROM), ICF 11, Turin, Italy, 2005.

[38] Yang, Y., M. D. Lepech, E. H. Yang, and V.C. Li, "Autogenous Healing of Engineering Cementitious Composites Under Wet-Dry Cycles," *Cem. Concr. Res.* Vol. 39, 2009, pp. 382–390.

[39] Wang, K., Jansen, D., Shah, S., and Karr, A., "Permeability Study of Cracked Concrete," *Cem.*

Concr. Res., Vol. 27, 1997, pp. 381–393.

[40] Evardsen, C., "Water Permeability and Autogenous Healing of Cracks in Concrete," *ACI Mater. J.*, Vol. 96, 1999, pp. 448–454.

[41] Reinhardt, H. W., and Jooss, M., "Permeability and Self-Healing of Cracked Concrete as a Function of Temperature and Crack Width," *Cem. Concr. Res.*, Vol. 33, 2003, pp. 981–985.